


# Hydratable Core–Shell Polymer Networks for Atmospheric Water Harvesting Powered by Sunlight

## Journal Article

### Author(s):

Maity, Debasis ; Teixeira, Ana Palma; Fussenegger, Martin 

### Publication date:

2023-11-22

### Permanent link:

<https://doi.org/10.3929/ethz-b-000626497>

### Rights / license:

[Creative Commons Attribution-NonCommercial 4.0 International](#)

### Originally published in:

Small 19(47), <https://doi.org/10.1002/smll.202301427>

### Funding acknowledgement:

785800 - Electrogenetics - Shaping Electrogenetic Interfaces for Closed-Loop Voltage-Controlled Gene Expression (EC)

# Hydratable Core–Shell Polymer Networks for Atmospheric Water Harvesting Powered by Sunlight

Debasis Maity, Ana Palma Teixeira, and Martin Fussenegger\*

The development of technologies to enable fresh water harvesting from atmospheric moisture could help overcome the problem of potable water scarcity. Here, an atmospheric water harvesting (AWH) device is assembled in a core–shell structure, with the core consisting of networks of alginate (Alg) and polyaniline (PANI) and the outer layer consisting of thermo-responsive poly(*N*-isopropylacrylamide) (PNIPAM) modified with sulfonic acid groups (SPNIPAM) to increase the water adsorption at low relative humidity. The resulting hydrogel, modified with lithium chloride (LiCl) for increased water storage capacity (SPNIPAM-Li-PANIALg), displays a similar lower critical solution temperature to pristine PNIPAM (32 °C) while affording a 15-fold higher water capture ratio, and releases water upon exposure to sunlight at intensities less than 1 kW m<sup>-2</sup>. The developed AWH system is capable of harvesting 6.5 L of water per kilogram in a single daily absorption/desorption cycle under sunlight and can operate at relative humidity levels as low as 17% with no additional external energy input. The thermo-responsive hydrogel SPNIPAM-Li-PANIALg exhibits excellent stability during natural sunlight-driven absorption/desorption cycles for at least 30 days, and allows sustainable harvesting of over 28.3 L kg<sup>-1</sup> from a moisture-rich environment by means of multiple absorption/desorption cycles.

to address the growing global challenge of water scarcity.<sup>[2–4]</sup> For example, sustainable and eco-friendly solar-powered vapor generation (SVG) can extract water from moist air or fog/dew.<sup>[5–8]</sup> However, the design of new materials with functional micro/nanostructures that absorb and convert low-intensity solar energy ( $\leq 1$  kW m<sup>-2</sup>) to heat for water phase transition is crucial for cost-effective water harvesting.<sup>[9–13]</sup> A radiative cooling system was recently designed to harvest atmospheric water (50 g m<sup>-2</sup> h<sup>-1</sup>) from dew under solar irradiation.<sup>[14]</sup>

Early atmospheric water-harvesting (AWH) devices employed economic and stable porous silica or zeolite materials, which absorb water molecules via hydrogen-bonding or electrostatic interactions. However, silica adsorbents suffer from low capacity at low relative humidity (RH),<sup>[15]</sup> while zeolites require high temperatures for regeneration/water desorption (150–200 °C).<sup>[16]</sup> More recently, highly porous metal-organic frameworks (MOFs) have attracted interest for AWH, as they feature favorable S-shaped water


sorption isotherms, have high adsorption capacity, and can be efficiently regenerated at low temperatures.<sup>[17]</sup> For instance, a MOF-801-based device was shown to be able to harvest 2.8 L of water per kilogram daily from the atmosphere at a flux of less than 1 sun (1 kW per m<sup>2</sup>).<sup>[6]</sup> However, the manufacture of MOFs is rather complex and costly, and their toxicity has not yet been fully investigated.<sup>[18]</sup>

A promising alternative to MOF-based systems is provided by hydrogels, which are physically or chemically cross-linked networks of different polymers with a porous capillary structure, that show excellent water collecting and releasing ability.<sup>[5,19–21]</sup> The weak bonds between the water molecules and the polymer network provide good SVG behavior due to the low energy requirement for water vaporization.<sup>[9,22,23]</sup> For instance, polyacrylamide (PAM) and alginate (Alg) matrix-based hydrogels were designed and fabricated as an AWH system for rapid adsorption and subsequent sunlight-activated desorption of water (1.81 kg kg<sup>-1</sup> m<sup>-2</sup> day<sup>-1</sup> at 23 °C, 66% RH).<sup>[24]</sup> Furthermore, a combination of graphene oxide (GO) with temperature-responsive poly(*N*-vinylcaprolactam-*co*-acrylic acid) copolymeric nanofibers enabled water capture and release based on hydrophilic-to-hydrophobic transformation across broad ranges of RH and temperature.<sup>[25]</sup> Other hydrogel-based systems include a photo-thermal device

## 1. Introduction

Atmospheric moisture represents a large-scale source of fresh water that is continuously replenished via the hydrologic cycle.<sup>[1]</sup> Therefore, capturing water from the air by means of rapid and energy-efficient techniques could be an effective approach

D. Maity, A. P. Teixeira, M. Fussenegger  
Department of Biosystems Science and Engineering  
ETH Zurich  
Mattenstrasse 26, Basel CH-4058, Switzerland  
E-mail: fussenegger@bsse.ethz.ch  
M. Fussenegger  
Faculty of Science  
University of Basel  
Mattenstrasse 26, Basel CH-4058, Switzerland

 The ORCID identification number(s) for the author(s) of this article can be found under <https://doi.org/10.1002/smll.202301427>

© 2023 The Authors. Small published by Wiley-VCH GmbH. This is an open access article under the terms of the Creative Commons Attribution-NonCommercial License, which permits use, distribution and reproduction in any medium, provided the original work is properly cited and is not used for commercial purposes.

DOI: 10.1002/smll.202301427

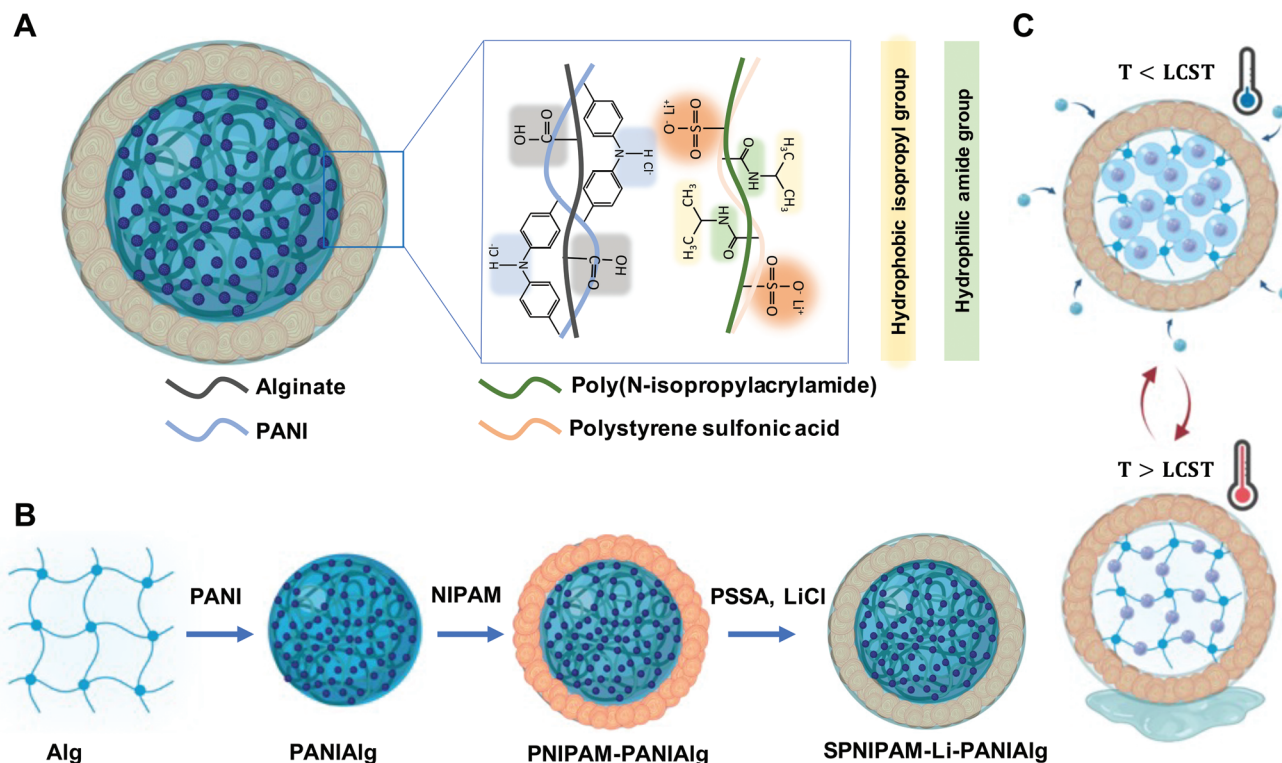


**Figure 1.** The design concept of our AWH system. A) Schematic illustration of a cross-section of the SPNIPAM-Li-PANIAlg hydrogel showing the core-shell structure. B) Schematic illustration of the synthetic procedure of SPNIPAM-Li-PANIAlg. The hydrogel is a hyper-crosslinked polymeric network composed of alginate (Alg), PANI, PNIPAM, sulfonate groups (PSSA), and LiCl. C) Schematic illustration of reversible water vapor sorption below the LCST and desorption above the LCST by the developed AWH hydrogel.

combining polydopamine and  $\text{Cl}^-$ -doped polypyrrole,<sup>[26]</sup> and a poly(vinyl alcohol) and activated carbon device,<sup>[27]</sup> achieving water evaporation rates of 1.43 and 2.6  $\text{kg m}^{-2} \text{h}^{-1}$  at 1 sun ( $1 \text{ kW m}^{-2}$ ), respectively.

Thermo-responsive poly(*N*-isopropylacrylamide) (PNIPAM) hydrogels have attracted particular attention because of their lower critical solution temperature (LCST) of just 32 °C,<sup>[28]</sup> resulting in easily switchable hydrophilicity using a low-energy consumption method.<sup>[29]</sup> A photosensitive porous system composed of carbon dots (C-dots), carboxymethylcellulose, and PNIPAM-based hydrogel<sup>[23]</sup> with ON/OFF optical switching was reported for solar-powered water purification, while PNIPAM grafted to silica gel was fabricated to obtain a high-performance thermo-responsive composite with an adsorption capacity of 1.70  $\text{g g}^{-1}$  at 20 °C and 70% RH.<sup>[30]</sup> In addition, the phase-transition and thermo-responsive properties of dried PNIPAM and hydrophilic Alg hybrid networks were investigated to improve water harvesting.<sup>[22]</sup> However, the thermo-responsiveness and water storage and release characteristics so far reported still fall short of the requirements for practical application.

In the present work, we designed core-shell structured hydrogels with a core consisting of polyaniline (PANI) incorporated in a calcium-crosslinked Alg matrix, shelled with PNIPAM modified with sulfonic acid groups (SPNIPAM) to enhance the water absorbance at low RH,<sup>[31,32]</sup> and treated with lithium chloride (LiCl) to enhance the water storage capacity. The resulting

hydrogel, SPNIPAM-Li-PANIAlg, showed a water capture ratio 15-fold higher than pristine PNIPAM, presumably due to enhanced water transport through the porous polymer network, and it released water on exposure to sunlight at an intensity of less than  $1 \text{ kW m}^{-2}$ . Furthermore, SPNIPAM-Li-PANIAlg was compatible with multiple adsorption-desorption cycles per day and showed long-term durability. In addition, we validated the performance of SPNIPAM-Li-PANIAlg in an outdoor prototype device as proof of concept for AWH in a real-world environment.

## 2. Results

### 2.1. Design and Construction of AWH

We designed a polymeric hydrogel comprising Alg and PANI chains in the core to enhance the moisture absorption and storage capacity, surrounded by thermo-responsive PNIPAM chains, modified by incorporation of poly(4-styrenesulfonic acid) (PSSA) to enhance the water capture ratio and hygroscopic LiCl to further enhance the storage capacity (Figure 1A). The core-shell structure of this hydrogel, designated SPNIPAM-Li-PANIAlg, was prepared by sequential steps of polymerization (Figure 1B). The outer layer of PNIPAM and PSSA enlarges the hydrogel-air interface and serves as a pathway for water capture and release. The water molecules are adsorbed and liquefied on this outer shell layer of the hydrogel, aided by the hydrophilic sulfonate groups incorporated in PNIPAM, and then are captured by diffusion into

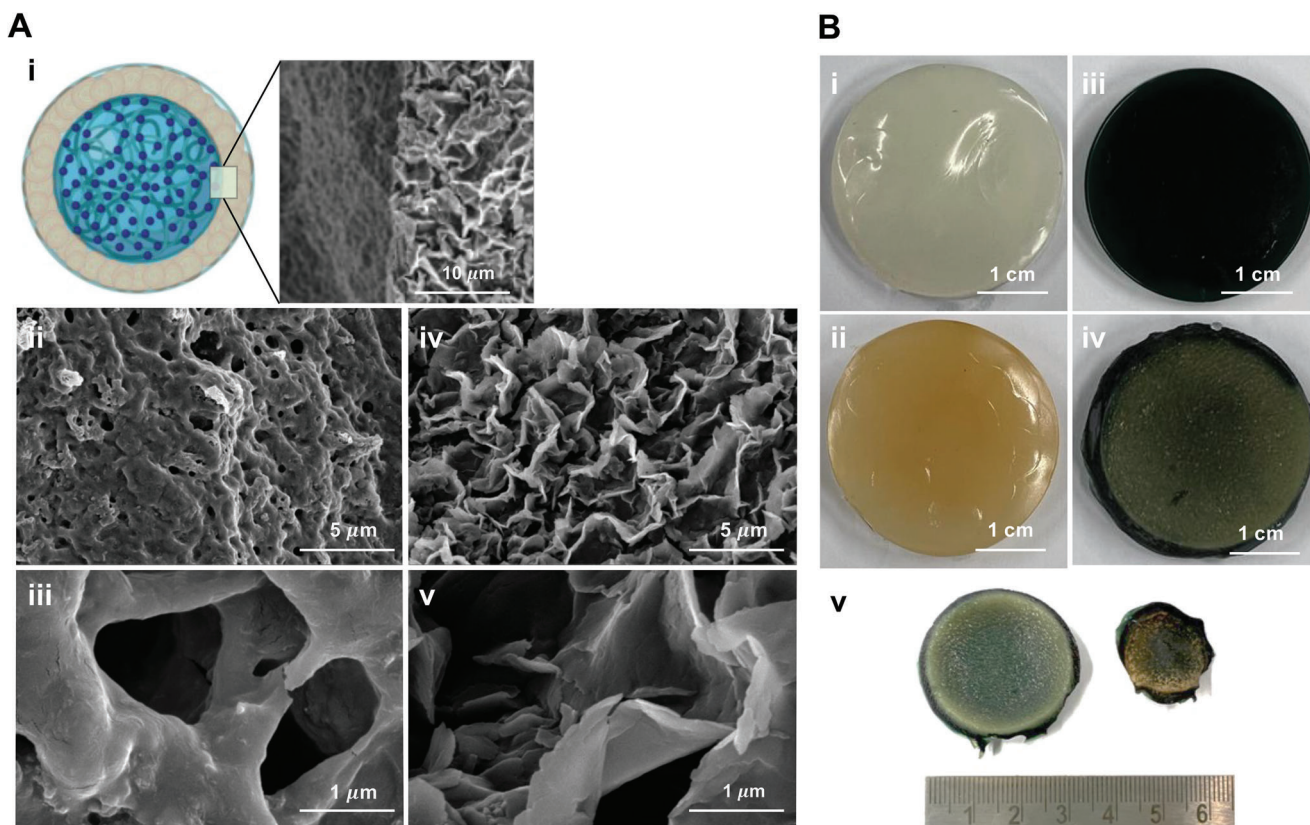


**Figure 2.** A) SEM images of the SPNIPAM-Li-PANiAlg hydrogel. i) Cross-sectional view from the top of a prepared disk. ii,iii) Images of the core part containing PANiAlg and iv,v) images of the shell part containing SPNIPAM (note the different magnifications). B) Photographs of i) Alg, ii) Alg with aniline monomer, iii) PANiAlg, and iv) SPNIPAM-Li-PANiAlg. v) Picture of one dried and one hydrated hydrogel disk, showing a volume change consistent with a large water yield.

the polymeric network of Alg and PANI. The polymer network undergoes a transition from hydrophobic to hydrophilic below the LCST ( $\approx 32$  °C), enabling the absorption of water within the highly porous PANiAlg core layer, while above the LCST, the hydrophobic environment of PNIPAM results in release of water molecules (Figure 1C).

The microstructure and surface topography of SPNIPAM-Li-PANiAlg were characterized by scanning electron microscopy (SEM) (Figure 2A). A cross-section of the hydrogel reveals a core-shell structure. The outer layer presents a rough, flaky morphology (Figure 2A), as reported previously,<sup>[33]</sup> while in the inner layer, the integration of PANI nanoparticles into the Alg network produces pores with a size of around one micron that serves as micro-channels for water release (Figure 2A, Figure S1, Supporting Information). To verify the presence and distribution of elements across the prepared hydrogel disks, we performed energy-dispersive X-ray analysis (EDS). While oxygen, nitrogen, and chlorine were distributed all over the hydrogel, sulfur was present mostly in the shell (consistent with  $\text{SO}_3^-$ -modified PNIPAM), and calcium was located mainly in the core of the hydrogel (Figure S2, Supporting Information). The appearance of the disk-molded hydrogel changes through the four different stages of the fabrication process (Figure 2B). At temperatures below the LCST, the hybrid hydrogel absorbs water vapor, which gradually penetrates into the inner structures of the hydrogel and is

stored throughout the hydrophilic Li-PANiAlg network until saturation is reached. The size of the SPNIPAM-Li-PANiAlg hydrogel disks changes significantly from the saturated state at 24 °C to the state after release of the total water content by exposure to 40 °C (higher than the LCST) on a hot plate: the thickness decreased from 4 to 1.67 mm, and the average volume decreased from 4.67 to 0.61  $\text{cm}^3$  (Figure 2B). Rheological characterization of SPNIPAM-Li-PANiAlg confirmed the viscoelastic nature of the hydrogel (Figure S3, Supporting Information). Alg showed a gel-like behavior, with the storage modulus ( $G'$ ) always above the loss modulus ( $G''$ ).<sup>[33]</sup> The  $G''$  values were stable over the whole tested frequency range, while the  $G'$  values increased at frequencies above 100  $\text{rad s}^{-1}$ . The incorporation of PANI and PNIPAM had little impact on the viscoelastic properties of the hydrogel, indicating that these properties are mainly attributed to the presence of Alg.

We also analyzed the monomer conversions into PANI and PNIPAM polymers by proton NMR, obtaining conversion ratios of over 93% for both polymerization processes (Table S1 and Figure S4, Supporting Information).<sup>[34]</sup> The gel fractions at the different polymerization stages were also determined. While the gel fraction of the initial Alg hydrogel is 28%, this decreases to 11.4% after the incorporation of all the remaining components into the final SPNIPAM-Li-PANiAlg hydrogel (Table S2, Supporting Information).

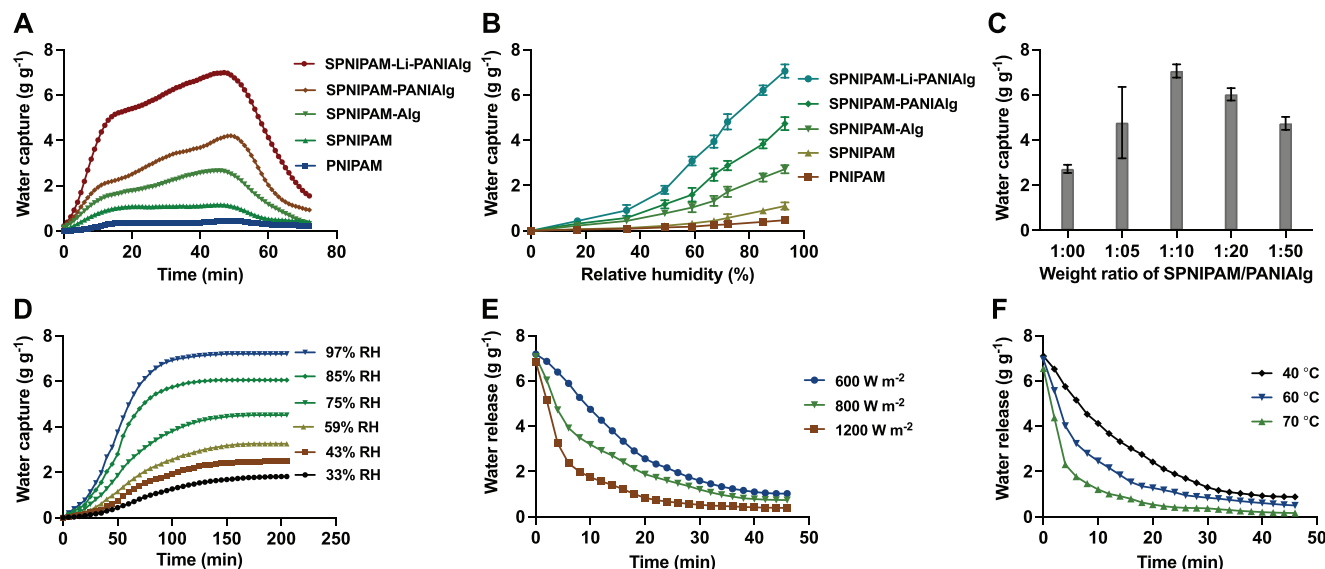


**Figure 3.** The natural moisture sorption properties of SPNIPAM-Li-PANIAlg. A) The water uptake and release of PNIPAM, SPNIPAM, SPNIPAM-Alg, SPNIPAM-PANIAlg, and SPNIPAM-Li-PANIAlg were gravimetrically profiled at a relative humidity (RH) of 93%. The water uptake was conducted at 24 °C (below the LCST), and water release at 60 °C (above the LCST). The hydrogel was loaded in a closed chamber with humid air flow for about 10 min, until the chamber reached the desired humidity. Then water release was initiated after 50 min of exposure. B) Calibration of moisture absorption kinetics study at 24 °C for different values of relative humidity (RH 17%, 35%, 49%, 59%, 67%, 72%, 85%, and 93%). C) Water capture of SPNIPAM-Li-PANIAlg with different mass ratios of shell (SPNIPAM) and core (PANIAlg) after 1 h of moisture uptake (24 °C, RH 93%). D) Water uptake of SPNIPAM-Li-PANIAlg over time at RH 33%, 43%, 59%, 75%, 85%, and 97%. This experiment was performed in a salt-solution-containing closed chamber with saturated humidity (without air flow). E) The dynamic water desorption process of SPNIPAM-Li-PANIAlg under light intensities of 600, 800, and 1200 W m<sup>-2</sup>. F) Moisture-desorption isotherms of hydrogel at different temperatures (40, 60, and 70 °C). Bars represent mean ± SEM, (n = 5).

## 2.2. Evaluation of Water Sorption Performance

To assess how the various components of the hydrogel impact the water vapor sorption properties, we compared the water uptake ratios at five different stages of hydrogel modification under 93% RH at 24 °C (Figure 3A). While pure PNIPAM has low hygroscopicity (0.44 g of water captured per g of material), the equilibrium water uptake is significantly increased by successively adding each of the remaining components, and the fully assembled hydrogel has excellent water sorption characteristics. The incorporation of the sulfonate groups increases the water uptake of PNIPAM by almost threefold (SPNIPAM, 1.16 g g<sup>-1</sup>). The microporous structure of Alg (SPNIPAM-Alg, 2.65 g g<sup>-1</sup>) and PANI (SPNIPAM-PANIAlg, 4.1 g g<sup>-1</sup>) provides effective moisture transport pathways and an enlarged contact area for moisture capture. Finally, the AWH performance of the fully assembled hydrogel was greatly enhanced by introducing LiCl solution, increasing the water capture capacity to 6.70 g g<sup>-1</sup>. LiCl reduces the saturated vapor pressure of water at the liquid-gas interface,<sup>[35]</sup> enhancing the driving force for water diffusion in the Alg-PANI matrix and thereby promoting faster moisture absorption and improving the moisture absorption capacity (Figure 3A). The free ions (Li<sup>+</sup> and Cl<sup>-</sup>) also facilitate the transfer of absorbed water molecules into the hydrogel core under a wide range of humid environments (Figure 3B).

Next, we assessed how the ability to capture water changes for hydrogels synthesized with different mass ratios of SPNIPAM to PANIAlg (Figure 3C). Increasing the concentration of PANIAlg versus SPNIPAM by 5- and 10-fold increased water absorption from 2.0 to 4.5 and 6.5 g g<sup>-1</sup>. However, when the concentration

of PANIAlg was further increased to 20- or 50-fold, the adsorption capacity decreased to 6 and 5 g g<sup>-1</sup>, respectively. This decay might be due to shrinkage of the macroscopic volume and microscopic pores. The as-prepared AWH hydrogels exhibited good water sorption capacity under a wide range of humidity (Figure 3D). The SPNIPAM-Li-PANIAlg hydrogel with a mass ratio of 10 (core/shell) was considered optimal. Notably, in 43% and 87% RH environments it took only around 100 and 75 min, respectively, for the SPNIPAM-Li-PANIAlg to reach 80% of equilibrium (Figure 3D). The water-harvesting was reduced significantly in the lower humidity range, but still amounted to 2 g g<sup>-1</sup> at 33% RH. The collected fresh water was analyzed by ion chromatography and all detected ions met the standards for potable water defined by the World Health Organization (Figure S5, Supporting Information).<sup>[36,37]</sup>

## 2.3. Evaluation of Water Desorption Performance

The LCST for the SPNIPAM-Li-PANIAlg hydrogel was 32 °C, which is the same as that of PNIPAM, despite the presence of Alg, PSSA, and PANI components, which enhance the hydrophilicity of the hydrogel (Figure S6, Supporting Information).<sup>[38]</sup> SPNIPAM-Li-PANIAlg exhibited excellent stability and retained 82% of its water-harvesting capacity after 30 days (Figure S7A, Supporting Information). Next, we carried out water release experiments after exposing SPNIPAM-Li-PANIAlg disks to a constant temperature of 24 °C and RH of 93% for 24 h. First, the photothermal responsiveness of SPNIPAM-Li-PANIAlg hydrogel was investigated using solar radiation focused with lenses to

achieve different light intensities of 0.6, 0.8, and 1.2 kW m<sup>-2</sup>. Although the hydrophobic nature of PNIPAM might present a barrier for the water stored in the core to diffuse throughout the shell, in practice we observed a rapid release during the first 5 min, and then the release slowed down as the water content decreased (Figure 3E). Higher light intensities produced faster water release rates. After 30 min of solar illumination, around 85–95% of the absorbed water was released from SPNIPAM-Li-PANIAAlg hydrogel, demonstrating the feasibility of water release powered by natural sunlight. The amount of water released at three different temperatures was also evaluated (Figure 3F). The surface temperature of the sample was increased from 24 °C to around 40, 60, and 70 °C respectively by means of a heating pad. Water release increased rapidly at temperatures above 40 °C, and more than 80% of the absorbed water was released within 15 min at 70 °C. However, SPNIPAM-Li-PANIAAlg shows impaired water-harvesting and storage properties at temperatures above 100 °C (Figure S7B, Supporting Information). The optimized amounts of aniline (50 μL) and LiCl (0.1 M) were used in further studies (Figure S8A,B, Supporting Information).

#### 2.4. Application of SPNIPAM-Li-PANIAAlg for Atmospheric Water Harvesting

For a proof-of-concept application in real-world conditions, a simple-to-install lens-assisted solar-powered-based water harvesting prototype device (Figure 4A) was deployed outside on the balcony of our department building, where sunlight fluxes in the range of 0.5 to 1 kW m<sup>-2</sup> are typically observed on sunny days. The device consists of three chambers, with the hydrogel disk hosted in the middle chamber, which has holes at the bottom to allow collected water to flow into the collection chamber under gravity. The top chamber contains a removable glass lens that focuses sunlight to assist water release. Figure 4B shows the result of a representative demonstration during the course of a day, in which the outdoor temperature and RH changed as shown, with an average incident solar flux of ≈0.7 sun. During humid periods, water was captured from the air at higher rates, reaching a maximum of 4.2 g of water per g of hydrogel (Figure 4C). In this device, the incident sunlight increases the temperature of the hydrogel to above 60 °C at an ambient temperature of 25 °C with the help of the lens, triggering the hydrophilic-to-hydrophobic phase transition of PNIPAM and prompting the accumulation of 2.1 grams of water per gram of hydrogel in the collection chamber.

Finally, we tested the capacity of the hydrogel to undergo several cycles per day. We set a period of 30 min for water sorption at 97% humidity and 15 min for desorption with an applied desorption temperature of 70 °C (Figure 4D). This protocol yielded 28.3 g of clean water per gram of SPNIPAM-Li-PANIAAlg after 8 absorption–desorption cycles.

### 3. Discussion

In this work, we designed and synthesized SPNIPAM-Li-PANIAAlg as a thermo-responsive hydratable polymer network for high-efficiency AWH. The fundamental design principle of

SPNIPAM-Li-PANIAAlg is to synergistically integrate a) sulfonate-modified PNIPAM for water absorption and liquefaction, b) photothermal conversion ability of PANI, c) hygroscopic Li-PANIAAlg for moisture storage, and d) a hydrophilicity switching and thermal response capability based on the PNIPAM network for rapid water release. The moisture absorption by the AWH device is a two-step process: i) the water molecules are adsorbed and liquefied on the surface of the sulfonic acid-modified PNIPAM, and ii) the condensed water is transferred to the PANIAAlg polymer network for storage.<sup>[35]</sup> The molecular structure of Alg includes six active hydrogen-bonding sites favorable for water storage.<sup>[39]</sup> The hygroscopic agent LiCl confers rapid water absorption and transport properties.<sup>[36]</sup>

Dried SPNIPAM in the shell part of the hydrogel absorbs moisture from air at temperatures below its LCST (32 °C). This process induces swelling of the hydrogel. PNIPAM-based hydrogels drastically change their polymer chain structure from hydrophilic to hydrophobic form in response to a small increase in temperature to above their LCST.<sup>[40]</sup> Thus, solar radiation can induce a volume phase transition at temperatures above the LCST, resulting in shrinkage of the swollen hydrogel and release of liquid water. In other words, the thermo-responsive hydrophilic/hydrophobic properties of PNIPAM and photothermal conversion of PANI provide an energy exchange system through which moisture from air can be condensed to liquid water with a small temperature change. This microporous super-hygroscopic hydrogel can deliver water at ≈6.34 L kg<sup>-1</sup> and can operate even in a very dry environment (≈17% RH).

The spongy morphology of the SPNIPAM-Li-PANIAAlg polymer network significantly influences water diffusion within the hydrogel and provides pathways for diffusion of water molecules to the evaporating surface.<sup>[41]</sup> The incorporation of hygroscopic LiCl and PANI in the hydrogel also increases its water-adsorbing capacity.<sup>[42]</sup> Overall, the core–shell configuration increases the input efficiency and provides pathways for water release with a low thermal energy requirement that can be provided by natural sunlight. Notably, SPNIPAM-Li-PANIAAlg showed a high water capture ratio (720% of that of PNIPAM), with a maximum evaporation rate of up to ≈2.35 L kg<sup>-1</sup> h<sup>-1</sup> (28.3 L kg<sup>-1</sup> over 12 h), together with the capability for multiple absorption and release cycles, owing to its high-capacity storage and conveniently controllable reversible phase transformation. The water capture performance of our fabricated AWH compares favorably with those of other recently developed AWH systems (Table S3, Supporting Information). Our design strategy highlights the potential of using core–shell configurations of different functional polymers for further developing advanced automated AWH systems with low power requirements and operability under dry conditions. We are planning further research to increase the moisture absorption over a wider range of temperature and humidity, to speed up the absorption and release processes, and to extend the long-term stability of the hydrogel.

### 4. Experimental Section

**Chemicals and Materials:** Chemicals including *N*-isopropylacrylamide (C<sub>6</sub>H<sub>11</sub>NO)<sub>n</sub> (cat. no. 2210-25-5), polystyrene sulfonic acid (cat. no. 28210-41-5), *N,N,N',N'*-tetramethylethylenediamine (cat. no. 3030-47-5),

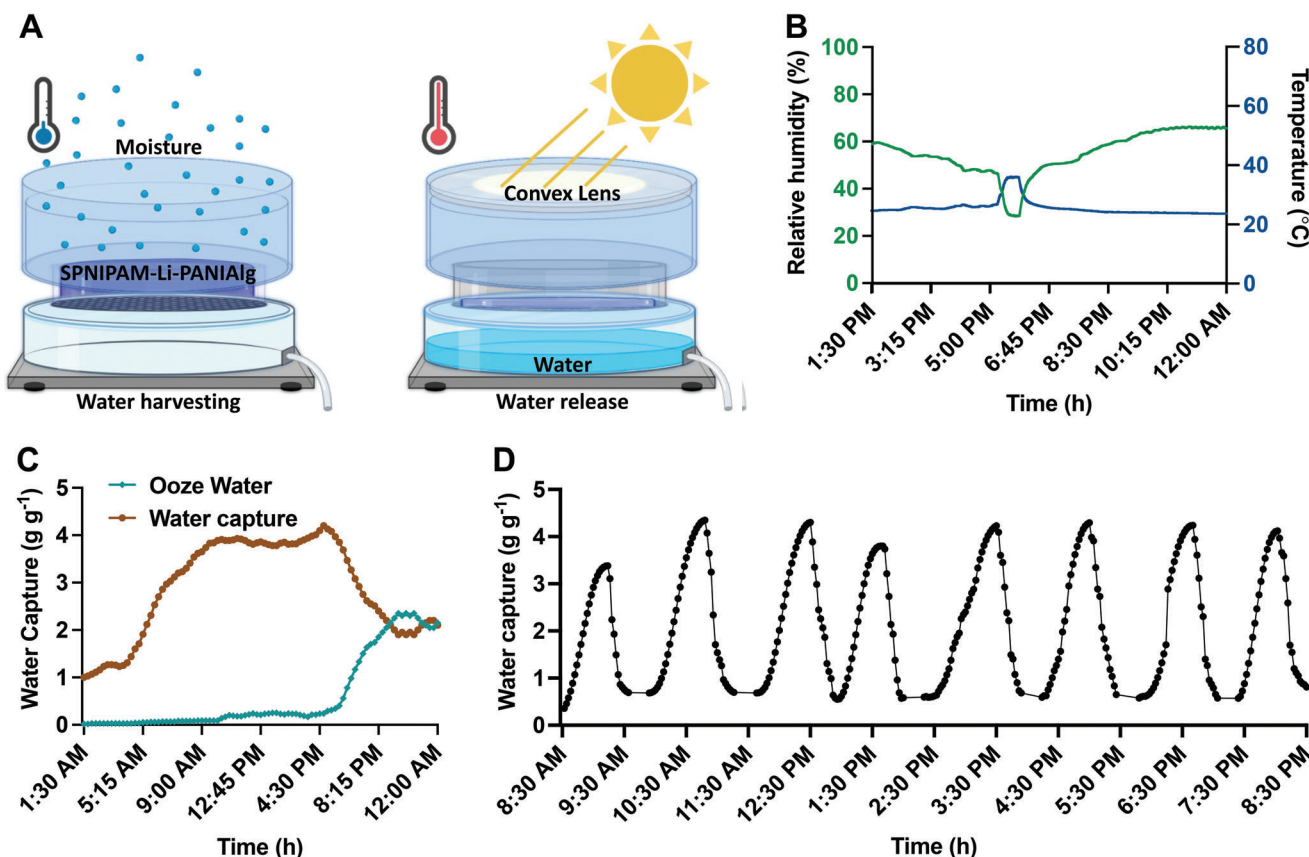


**Figure 4.** Outdoor testing of AWH performance under natural sunlight. A) Schematic illustration of a prototype built for field study of the absorption characteristics of the hydrogel. Schematic of a simple-to-use, solar-energy-based water collector prototype (20 cm × 15 cm × 15 cm) in water capture and water harvesting modes. B) The outdoor ambient temperature and humidity were recorded during a mostly sunny day from 1.30 PM to the next day at 00:00 h. C) SPNIPAM-Li-PANiAlg absorbs water and releases it under lens-mediated solar heating. Hygroscopic/evaporation experiment conducted from 1.30 PM to 00.00 AM. Water capture and release were recorded. D) Plot showing multiple cycles of water collection occurring in 1 day. The water sorption period was 30 min and the desorption period was 15 min at 97% humidity with an applied desorption temperature of 70 °C.

ammonium persulfate (APS, cat. no. 7727-54-0), *N,N'*-methylene-bis-acrylamide (cat. no. 110-26-9), aniline (cat. no. 62-53-3), lithium chloride (cas. no. 7447-41-8) and hydrochloric acid (cat. no. 7647-01-0) were purchased from Sigma Aldrich (Switzerland). Alg powder was purchased from Büchi (cat. no. 11061528; Büchi, Switzerland).

**Preparation of SPNIPAM-PANiAlgLi Hydrogel:** Alginate powder was dissolved in 50 mL of aqueous solution to a concentration of 2% w/w and stirred for 24 h to obtain a uniform solution, then sonicated for 10 min. A 50 µL aliquot of aniline monomer solution was mixed with the Alg solution by vortexing for 5 min and the resulting solution was labeled as solution A. Calcium chloride (0.1 M) was added dropwise to solution A contained in plastic disk molds of various sizes. The Alg solution was rapidly crosslinked with Ca<sup>2+</sup>, forming the core of the hydrogel (ANiAlg). ANiAlg was treated for 30 min with 100 µL of hydrochloric acid (HCl) solution (37%). Next, 1 mL of ammonium persulfate (0.1 M) was added dropwise and the mixture was allowed to polymerize for 1 h at 24 °C to form PANiAlg. The obtained PANiAlg hydrogel was immersed in water and ethanol alternately (five times) for 15 min to remove HCl, ammonium persulfate, and unreacted monomers. *N*-Isopropylacrylamide (NIPAM, 300 mg), *N,N,N',N'*-tetramethyl-ethylenediamine (100 µL) and Millipore water (10 mL) were mixed and the solution was purged with nitrogen for 30 min to remove oxygen. Bubbles were removed by centrifuging at 4000 rpm (5000 g), 10 °C for 4 min, and the resulting solution was named solution B. Solution B was added to the disk mold containing hydrogel (PANiAlg) for 4 h at 24 °C. A mixture of the crosslinker *N,N'*-methylene-bis-acrylamide (10% v/v) and initiator ammonium persulfate

(0.1 M) was prepared by vortexing and labeled as solution C. Solution C (10% v/v) was added to the above product and kept for 2 h at RT under a nitrogen flow (polymerization of PNIPAM was quenched by the dissolved oxygen in the water). The transparency of the Alginate was reduced by the whitish PNIPAM on the surface and black PANI (mostly in the core, Figure 2B-iv). The obtained PNIPAM-PANiAlg hydrogel was immersed in cold water (10 °C) and hot water (50 °C) alternately (eight times) for 3 h to remove unreacted monomers and non-crosslinked polymers. The product was washed with water four times to remove unattached NIPAM monomer. Next, polystyrene sulfonic acid was uniformly mixed with 20 mL ethanol (5% v/v) by sonication for 30 min and labeled as solution D. The PNIPAM-PANiAlg hydrogel was slowly immersed in solution D and kept for 24 h to get a uniform coating of polystyrene sulfonic acid (SPNIPAM-PANiAlg). This product was then immersed in 0.1 M LiCl solution to obtain SPNIPAM-Li-PANiAlg hydrogel, which was purified by washing with Millipore water five times. The monomer conversion percentage during polymerization was calculated from the results of NMR analysis (Figure S8 and Table S2, Supporting Information). The resulting SPNIPAM-Li-PANiAlg disks were completely dried in a vacuum chamber at 24 °C for 24 h. For water-harvesting, dried SPNIPAM-Li-PANiAlg disks (0.5 mg each) were exposed to moist air at a constant flow rate. To release the captured water, the SPNIPAM-Li-PANiAlg disks were heated by direct or convex-lens-assisted solar radiation. The SPNIPAM-Li-PANiAlg hydrogel absorption/release cycles at RH 17%, 29%, 45%, 60%, 75%, and 93% were run with capture and release times of 6 h and 30 min, respectively. In the case of multiple cycles in a day at RH 93%, the capture and release

times were 45 and 15 min. respectively (eight cycles). The rapid absorption and release experiment was performed at RH 93% with capture and release times of 20 and 10 min, respectively.

**Water Capture Experiments with Standard Calibration:** Completely dried samples of SPNIPAM-Li-PANIAIlg hydrogel were placed in a closed system in which the RH was controlled by the presence of saturated solutions of LiCl, magnesium chloride (MgCl<sub>2</sub>), potassium carbonate (K<sub>2</sub>CO<sub>3</sub>), sodium chloride (NaCl), potassium chloride (KCl) and potassium sulfate (K<sub>2</sub>SO<sub>4</sub>). These provide RH levels of 11%, 33%, 43%, 75%, 85%, and 97%, respectively. Humidity in the chamber was monitored with a humidity sensor.

**Water Release Experiments:** Hydrated SPNIPAM-Li-PANIAIlg hydrogel samples were placed in a glass petri dish and exposed to a heating pad or to direct solar radiation. The solar light intensity flux was measured using a thermopile (Newport, 818SL) connected to a power meter (Newport, 1916-R). The real-time surface temperature of SPNIPAM-Li-PANIAIlg hydrogel was measured by a non-contact infrared thermometer. The released water was weighed in a graduated cylinder. Water release from SPNIPAM-Li-PANIAIlg hydrogel was monitored in terms of weight change.

**Characterization:** The morphology and microstructure of the hydrogel samples were observed with a Zeiss GeminiSEM 450 field emission scanning electron microscope (ZEISS, Oberkochen, Germany). The surface temperature of the composite hydrogel was measured with an IR thermometer (Fluke VT04). Before observation, the hydrogels were freeze-dried for 24 h. The humidity and temperature were measured with a commercial humidity and temperature data logger (RS PRO 1365, RS Components Ltd., Northamptonshire, UK). Elemental mapping analysis of the hydrogel was done by energy-dispersive X-ray spectroscopy using a Zeiss GeminiSEM 450. Rheological measurements of the hydrogel were carried out using a rotational MCR 302 rheometer (Anton Paar, Graz, Austria), equipped with a parallel plate (pp25 and pp50) geometry. To determine the gel fractions, the pre-weighed samples were dried under vacuum at room temperature to check for changes in weight. The samples were soaked in water for 4 days and then collected and dried under vacuum at room temperature until their weight remained constant.<sup>[43,44]</sup>

Gel fraction (%) =  $\frac{W'}{W^0}$ ; where  $W'$  refers to the weight of the dried sample and  $W^0$  is the weight of the soaked sample. NMR was conducted to analyze the monomer-to-polymer conversion efficiency, using sodium formate (HCOONa) as a standard sample.<sup>[34]</sup> The <sup>1</sup>H NMR analysis was performed in a Bruker Avance III HD instrument (Switzerland) operating at 500 MHz, using a 5-mm BBFO smart probe equipped with actively shielded z-gradients (10 A). The experiments were performed at 298 K. The thermoresponsive behavior of aqueous solutions (10% v/v) of PNIPAM and SPNIPAM-Li-PANIAIlg was studied by measuring how the transmittance at 460 nm changed with temperature. The temperature at which the transmittance was 90% of the initial value (at 20 °C) was defined as the LCST.<sup>[45,46]</sup>

**Water Quality Analysis:** The quality of the water was analyzed by ion chromatography (IC 940 von Metrohm, Switzerland) with a 30 min cycle time and 1 mL min<sup>-1</sup> flow rate.

**Statistical Analysis:** All data sets were analyzed using GraphPad Prism software (version 8.4.3, La Jolla, CA, USA), following a two-way ANOVA *t*-test. All experiment data are presented as mean ± standard deviation (SD) for *n* = 5 as noted in the figure legends.

## Supporting Information

Supporting Information is available from the Wiley Online Library or from the author.

## Acknowledgements

The authors thank Ivan Cornu for NMR spectroscopy, Guy Seltensperger for ion chromatography, Zarah Korb for rheological characterizations, and Jikson Pulparayil Mathew for generous advice. This work was financially

supported through a European Research Council advanced grant (ElectroGene, no. 785800) and in part by the Swiss National Centre of Competence in Research Robotics (NCCR) for Molecular Systems Engineering.

Open access funding provided by Eidgenössische Technische Hochschule Zurich.

## Conflict of Interest

The authors declare no conflict of interest.

## Author Contributions

D.M., A.P.T., and M.F. designed the project, analyzed the results, and wrote the manuscript.

## Data Availability Statement

The data that support the findings of this study are available from the corresponding author upon reasonable request.

## Keywords

harvesting water, moisture, temperature, thermo-responsive hydrogels

Received: February 16, 2023

Revised: July 17, 2023

Published online: July 31, 2023

- [1] T. Oki, S. Kanae, *Science* **2006**, *313*, 1068.
- [2] M. M. Mekonnen, A. Y. Hoekstra, *Sci. Adv.* **2016**, *2*, e1500323.
- [3] A. A. Salehi, M. Ghannadi-Maragheh, M. Torab-Mostaedi, R. Torkaman, M. Asadollahzadeh, *Renewable Sustainable Energy Rev.* **2020**, *120*, 109627.
- [4] J. Lord, A. Thomas, N. Treat, M. Forkin, R. Bain, P. Dulac, C. H. Behroozi, T. Mamutov, J. Fongheiser, N. Kobilansky, S. Washburn, C. Truesdell, C. Lee, P. H. Schmaelzle, *Nature* **2021**, *598*, 611.
- [5] X. Zhou, F. Zhao, Y. Guo, B. Rosenberger, G. Yu, *Sci. Adv.* **2019**, *5*, eaaw5484.
- [6] H. Kim, S. R. Rao, E. A. Kapustin, L. Zhao, S. Yang, O. M. Yaghi, E. N. Wang, *Nat. Commun.* **2018**, *9*, 1191.
- [7] D. K. Nandakumar, S. K. Ravi, Y. Zhang, N. Guo, C. Zhang, S. C. Tan, *Energy Environ. Sci.* **2018**, *11*, 2179.
- [8] F. Zhao, X. Zhou, Y. Shi, X. Qian, M. Alexander, X. Zhao, S. Mendez, R. Yang, L. Qu, G. Yu, *Nat. Nanotechnol.* **2018**, *13*, 489.
- [9] D. K. Nandakumar, Y. Zhang, S. K. Ravi, N. Guo, C. Zhang, S. C. Tan, *Adv. Mater.* **2019**, *31*, 1806730.
- [10] J. Xu, T. Li, J. Chao, S. Wu, T. Yan, W. Li, B. Cao, R. Wang, *Angew. Chem., Int. Ed.* **2020**, *59*, 5202.
- [11] J. Ju, H. Bai, Y. Zheng, T. Zhao, R. Fang, L. Jiang, *Nat. Commun.* **2012**, *3*, 1246.
- [12] M. Wang, T. Sun, D. Wan, M. Dai, S. Ling, J. Wang, Y. Liu, Y. Fang, S. Xu, J. Yeo, H. Yu, S. Liu, Q. Wang, J. Li, Y. Yang, Z. Fan, W. Chen, *Nano Energy* **2021**, *80*, 105569.
- [13] A. LaPotin, Y. Zhong, L. Zhang, L. Zhao, A. Leroy, H. Kim, S. R. Rao, E. N. Wang, *Joule* **2021**, *5*, 166.
- [14] K. K. Hyunho, S. Yang, S. Narayanan, E. A. Kapustin, H. Furukawa, A. S. Umans, O. M. Yaghi, E. N. Wang, *Science* **2017**, *434*, 430.



- [15] C. X. Jia, Y. J. Dai, J. Y. Wu, R. Z. Wang, *Energy Convers. Manage.* **2006**, 47, 2523.
- [16] A. Krajnc, J. Varlec, M. Mazaj, A. Ristić, N. Z. Logar, G. Mali, *Adv. Energy Mater.* **2017**, 7, 1601815.
- [17] W. Xu, O. M. Yaghi, *ACS Cent. Sci.* **2020**, 6, 1348.
- [18] N. Hanikel, M. S. Prévot, O. M. Yaghi, *Nat. Nanotechnol.* **2020**, 15, 348.
- [19] A. Entezari, M. Ejeian, R. Wang, *Appl. Therm. Eng.* **2019**, 161, 114109.
- [20] J. Yang, X. Chen, J. Zhang, Y. Wang, H. Wen, J. Xie, *Int. J. Biol. Macromol.* **2021**, 189, 53.
- [21] X. Zhou, Y. Guo, F. Zhao, G. Yu, *Acc. Chem. Res.* **2019**, 52, 3244.
- [22] K. Matsumoto, N. Sakikawa, T. Miyata, *Nat. Commun.* **2018**, 9, 2315.
- [23] S. Singh, R. Jelinek, *ACS Appl. Polym. Mater.* **2020**, 2, 2810.
- [24] H. Park, I. Haechler, G. Schnoering, M. D. Ponte, T. M. Schutzius, D. Poulidakos, *ACS Appl. Mater. Interfaces* **2022**, 14, 2237.
- [25] S. Kim, Y. Liang, S. Kang, H. Choi, *Chem. Eng. J.* **2021**, 425, 131601.
- [26] F. Ni, P. Xiao, N. Qiu, C. Zhang, Y. Liang, J. Gu, J. Xia, Z. Zeng, L. Wang, Q. Xue, T. Chen, *Nano Energy* **2020**, 68, 104311.
- [27] Y. Guo, F. Zhao, X. Zhou, Z. Chen, G. Yu, *Nano Lett.* **2019**, 19, 2530.
- [28] S. Lanzalaco, E. Armelin, *Gels* **2017**, 3, 36.
- [29] A. Graillot, D. Bouyer, S. Monge, J. J. Robin, C. Faur, *J. Hazard. Mater.* **2013**, 244, 507.
- [30] Q. Ma, X. Zheng, *Chem. Eng. J.* **2022**, 429, 132498.
- [31] D. Maity, M. Fussenegger, *Adv. Science* **2023**, 2300750.
- [32] P. Thuéry, Y. Atoini, J. Harrowfield, *Dalton Trans.* **2019**, 48, 8756.
- [33] P. Sánchez-Cid, M. Jiménez-Rosado, V. Perez-Puyana, A. Guerrero, A. Romero, *Polymers* **2021**, 13, 632.
- [34] J. U. Izunobi, C. L. Higginbotham, *J. Chem. Educ.* **2011**, 88, 1098.
- [35] C. D. Díaz-Marín, L. Zhang, Z. Lu, M. Alshrah, J. C. Grossman, E. N. Wang, *Nano Lett.* **2022**, 22, 1100.
- [36] W. Yao, X. Zhu, Z. Xu, R. A. Davis, G. Liu, H. Zhong, X. Lin, P. Dong, M. Ye, J. Shen, *ACS Appl. Mater. Interfaces* **2022**, 14, 4680.
- [37] S. Aleid, M. Wu, R. Li, W. Wang, C. Zhang, L. Zhang, P. Wang, *ACS Mater. Lett.* **2022**, 4, 511.
- [38] R. Kanno, M. Ouchi, T. Terashima, *Polym. Chem.* **2023**, 14, 1718.
- [39] A. Entezari, M. Ejeian, R. Wang, *ACS Mater. Lett.* **2020**, 2, 471.
- [40] F. Zhao, X. Zhou, Y. Liu, Y. Shi, Y. Dai, G. Yu, *Adv. Mater.* **2019**, 31, 1806446.
- [41] J. Xu, T. Li, T. Yan, S. Wu, M. Wu, J. Chao, X. Huo, P. Wang, R. Wang, *Energy Environ. Sci.* **2021**, 14, 5979.
- [42] M. Canales, D. Aradilla, C. Alemán, *J. Polym. Sci., Part B: Polym. Phys.* **2011**, 49, 1322.
- [43] S. N. Kim, S. C. Shim, D. Y. Kim, Y. H. Rhee, Y. B. Kim, *Macromol. Rapid Commun.* **2001**, 22, 1066.
- [44] N. Gull, S. M. Khan, M. T. Z. Butt, S. Khalid, M. Shafiq, A. Islam, S. Asim, S. Hafeez, R. U. Khan, *RSC Adv.* **2019**, 9, 31078.
- [45] M. F. Ji, X. J. Qiu, L. Hou, S. N. Huang, Y. M. Li, Y. Liu, S. F. Duan, Y. R. Hu, *Int. J. Nanomed.* **2018**, 13, 1773.
- [46] S. Ida, Y. Toyama, S. Takeshima, S. Kanaoka, *Polym. J.* **2020**, 52, 359.